



A universal approach to predicting temperature response of metallic parts to spray quenching

ISSAM MUDAWAR† and THOMAS A. DEITERS

Boiling and Two-Phase Flow Laboratory, School of Mechanical Engineering,
Purdue University, West Lafayette, IN 47907, U.S.A.

(Received 4 June 1993 and in final form 27 August 1993)

Abstract—A new method was developed to predict the temperature response of metallic parts to spray quenching below the film boiling regime. Local heat flux measurements in surfaces subjected to full cone and hollow cone sprays revealed existing correlations based on local values of volumetric spray flux, Sauter mean diameter, and mean drop velocity are both accurate and spatially independent in the transition boiling and nucleate boiling regimes, but less accurate in the single-phase regime due to liquid run-off effects. It is shown how the instantaneous spatial distribution of the heat transfer coefficient can be predicted from a mapping of the spatial distributions of the spray hydrodynamic parameters. The validity of this approach is demonstrated by comparing numerical predictions to the temperature response of a large rectangular aluminum block subjected on one surface to a nonuniform water spray. It is shown that the new method is universally applicable to sprays having drastically different patterns.

1. INTRODUCTION

SPRAY QUENCHING is used extensively in the heat treating of aluminum, steel and other metallic alloys. A spray consists of a dispersion of fine drops formed by either supplying liquid at high pressure through a small orifice (plain orifice spray) or by assisting liquid breakup with a high pressure supply of air (atomized spray). Liquid breakup results in a drastic increase in particle (drop) interfacial area to volume ratio. The combination of small particle size and large impact speed are key attributes of spray cooling, resulting in significant increases in cooling effectiveness per flow rate over other cooling techniques. Atomizers are commonly employed in the cooling of steel while plain orifice sprays are more popular in the aluminum industry. The present study is concerned with plain-orifice spray cooling.

Heat treating is a three step process, *solution heat treating*, *quenching*, and *age hardening*, designed to alter the metallurgical structure of alloys for the purpose of enhancing mechanical properties such as hardness and yield strength. During solution heat treating, the part is heated to a temperature exceeding the solvus but below the liquidus, dissolving the alloying elements within the primary metal crystal structure. Following solution heat treating, rapid quenching to room temperature ensures that the soluble elements are retained in a supersaturated solid solution with minimal precipitation. Age hardening consists of reheating the alloy following quenching to some intermediate temperature below the solvus for several hours to promote a fine dispersion of the precipitates

within the crystals of the primary metal. Fine dispersion allows the precipitates to resist deformation, thus enhancing both hardness and strength. If the quenching proceeds at a slow rate, massive precipitation will occur along the crystal boundaries rather than within the crystals themselves. The resulting alloy in this case is one which is not age-hardenable during subsequent reheating. Thus, the cooling rate must exceed some minimum value, which depends on the size and shape of the part, if proper heat treating is to take effect.

While rapid cooling is essential for enhancing hardness and strength, it can often result in serious adverse effects such as warping, cracking, and concentration of residual stresses, especially with parts having cross sections with large variations in thickness (i.e. thermal mass). Consequently, an optimum *cooling window* exists for every metallic part below which cooling rate would be insufficient to suppress precipitation and above which unacceptably large stresses would develop. Quenching which results in conditions outside the cooling window is largely responsible for both the massive amounts of alloy scrap produced worldwide and the costly post treatment and mechanical straightening often required to bend parts back to the desired shape. Interestingly, it is well acknowledged in the aluminum industry that over 50% of the production cost of aluminum extrusions is associated with post treatment due to the warping and concentration of stresses thermally induced during quenching. Therefore, in order to improve quality and consistency between production runs and to reduce cost, a method for optimizing the cooling rate for a particular part shape and composition is needed. The development of such a method requires that the cooling characteristics of sprays be fully predictable. This need

† Author to whom all correspondence should be addressed.

NOMENCLATURE

| | | | |
|------------------------|--|------------------|---|
| A_0, A_1, \dots, A_5 | empirical constants | Z | distance perpendicular to quenched surface of aluminum block. |
| c_p | specific heat | Greek symbols | |
| d_{32} | Sauter mean diameter (SMD) | α | thermal diffusivity of solid |
| h | heat transfer coefficient | ΔT_s | $T_s - T_f$ |
| h_{fg} | latent heat of vaporization | ΔT_{sub} | $T_{sat} - T_f$ |
| k | thermal conductivity | ν | kinematic viscosity |
| l | nozzle-to-surface distance | ρ | density |
| Nu | Nusselt number, hd_{32}/k_f | σ | surface tension |
| P | nozzle upstream gauge pressure | ψ | spatial distribution function. |
| Pr | Prandtl number | Subscripts | |
| q'' | heat flux | f | liquid |
| q''_{max} | critical heat flux | g | vapor |
| Q'' | volumetric spray flux | max | critical heat flux (CHF) |
| Re | Reynolds number, $Q''d_{32}/\nu_f$ | o | initial condition |
| t | time | s | surface |
| T | temperature | sat | saturation |
| U_m | mean drop velocity | sub | subcooled. |
| X | distance measured along length of quenched surface of aluminum block | | |
| Y | distance measured along width of quenched surface of aluminum block | | |

has spurred several cross-disciplinary efforts, involving thermal, metallurgical, and chemical aspects of heat treating which culminated in a CAD-based intelligent materials processing system described in a previous paper by the authors [1].

As a metallic part is quenched, whether by a spray or in a stagnant liquid bath, its surface experiences four different heat transfer regimes: film boiling, transition boiling, nucleate boiling, and single-phase liquid cooling. These regimes are identified with the aid of the boiling curve. Due to the relatively high solution heat treatment temperature, quenching of most metallic surfaces often commences in the film boiling regime. Despite a momentary contact of liquid with the surface at the instant of drop impact, a thermally insulating vapor layer quickly develops on the surface, resulting in a relatively slow cooling process. Better liquid-surface contact is maintained once the surface temperature drops below the minimum heat flux point. In the transition regime, liquid maintains partial contact with the surface in regions undergoing intense boiling while other regions remain insulated with vapor. The intermittent contact in the transition boiling regime greatly accelerates the cooling relative to the film boiling regime. In the nucleate boiling regime, the entire surface becomes available for liquid-surface contact which, along with the ensuing vigorous bubble production, accelerates the cooling further. Quenching is concluded in the slow, single-phase liquid cooling regime where the wall superheat becomes too weak to sustain bubble nucleation.

Spray cooling literature

The literature includes numerous studies concerning spray cooling as it applies to steel making.

Most of these studies explored means of predicting the heat transfer coefficients at the high surface temperatures associated with steel making which fall in the film boiling regime. A comprehensive review of these studies by Brimacombe *et al.* [2] revealed volumetric spray flux, Q'' , has the greatest influence on the heat transfer coefficient. However, there are many disagreements among investigators concerning the effects of other parameters. Some, for example, suggested the effect of surface temperature is negligible in the film boiling regime [3, 4], others disagree [5, 6]. Other parameters which have been suggested to influence the spray heat transfer coefficient include nozzle exit velocity [6] and distance of the nozzle from the surface [7].

Prediction of the heat transfer coefficient in spray cooling is complicated by another factor widely overlooked in the literature, spatial variation of spray hydrodynamic parameters within the spray field. As an example, Urbanovich *et al.* [7] and Reiners *et al.* [8] found that the practice of moving the spray nozzle closer to the surface, in order to increase the heat transfer coefficient, often resulted in severe spatial non-uniformity in cooling rate.

As mentioned earlier, most studies of spray quenching have been concerned with the cooling of steel from very high temperatures and, consequently, the conclusions drawn from these studies pertain largely to the film boiling regime. However, there are many other alloys (e.g. aluminum) for which the temperatures influencing the metallurgical structure range from just above the Leidenfrost point to well into the nucleate boiling regime. Recently, Mudawar and Valentine [9] explored means of determining the heat transfer coefficient in transition boiling, nucleate boil-

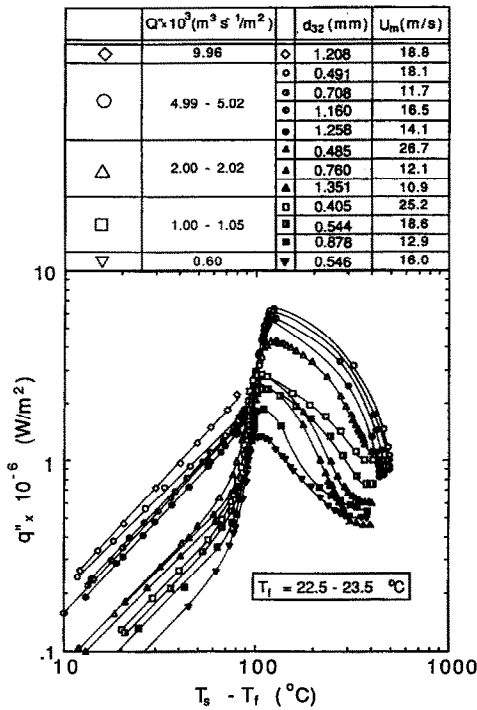


FIG. 1. Spray cooling curves for different values of volumetric spray flux, Sauter mean diameter, and mean drop velocity adapted from Mudawar and Valentine [9].

ing, and single-phase cooling regimes. They determined that, for their correlations to apply to different types of sprays and to different nozzle-to-surface distances, these correlations had to be based on spray parameters just prior to impingement upon the surface. Aside from surface temperature, they isolated three other parameters as influencing, to various degrees depending on boiling regime, the local heat flux: volumetric spray flux, Q'' , Sauter mean diameter,

d_{32} , and mean drop velocity, U_m . The resulting heat transfer correlations were based on measurements made at the geometrical center of each spray. While the heat transfer coefficient was very sensitive to variations in volumetric flux, mean drop velocity was also important in the transition boiling regime and Sauter mean diameter in the single-phase regime as depicted in Fig. 1. In the nucleate boiling regime, the heat transfer coefficient was a function of surface temperature alone, unaffected by variations in any of the spray hydrodynamic parameters. Mudawar and Valentine also demonstrated that (1) the boiling curve associated with transient spray quenching is identical to that determined from steady-state measurements and (2) the spray boiling curve is insensitive to the type of metallic surface used in the measurements. A summary of the Mudawar and Valentine correlations is given in Table 1.

The authors of the present study performed extensive measurements of the heat transfer coefficient across a nonuniform spray field, Fig. 2(a), using a local heat flux measurement probe, to be described in the next section, which was translated across the spray field. As shown in Fig. 2(b), the heat transfer coefficient appears to follow a Gaussian distribution with respect to each of the X and Y directions following, predominantly, the distribution of volumetric spray flux for the type of nozzle used. These results posed the following questions concerning the prediction of the spatial distribution of the spray heat transfer coefficient in determining the temperature response of metallic parts to spray quenching:

- (1) Could existing correlations which were determined at the geometrical center of a spray be used elsewhere in the spray field?
- (2) What is the most effective means of accounting for the spatial variations of the spray hydrodynamic

Table 1. Summary of Mudawar and Valentine's spray cooling correlations [9]

| Boiling (quenching) regime | Correlation |
|------------------------------|---|
| Transition boiling regime | $\log_{10} \left(\frac{q''}{q''_{\max}} \right) = 4.78 \times 10^5 \left(\frac{U_m}{Q''} \right)^{-1.255} \left(\log_{10} \left(\frac{T_s - T_f}{T_{\max} - T_f} \right) \right)^3$ $- 1.90 \times 10^4 \left(\frac{U_m}{Q''} \right)^{-0.903} \left(\log_{10} \left(\frac{T_s - T_f}{T_{\max} - T_f} \right) \right)^2$ |
| Critical heat flux | $\frac{q''_{\max}}{\rho_g h_{fg} Q''} = 122.4 \left[1 + 0.0118 \left(\frac{\rho_f}{\rho_g} \right)^{1/4} \left(\frac{\rho_f c_{p,f} \Delta T_{\text{sub}}}{\rho_g h_{fg}} \right) \right] \left(\frac{\sigma}{\rho_f Q''^2 d_{32}} \right)^{0.198}$ $T_{\max} = 18 \left[(\rho_g h_{fg} Q'') \left(\frac{\sigma}{\rho_f Q''^2 d_{32}} \right)^{0.198} \right]^{1/5.55} + T_f$ |
| Nucleate boiling regime | $q'' = 1.87 \times 10^{-5} (T_s - T_f)^{5.55}$ |
| Onset of single-phase regime | $T_s = 13.43 Re^{0.167} Pr_f^{0.123} \left(\frac{k_f}{d_{32}} \right)^{0.220} + T_f$ |
| Single-phase regime | $Nu = 2.512 Re^{0.76} Pr_f^{0.56}$ |

Units of the parameters are: q'' [W m^{-2}], T [K], Q'' [$\text{m}^3 \text{ s}^{-1} \text{ m}^{-2}$], U_m [m s^{-1}], d_{32} [m], k_f [$\text{W m}^{-1} \text{ K}^{-1}$], ρ_f [kg m^{-3}], ρ_g [kg m^{-3}], $c_{p,f}$ [$\text{J kg}^{-1} \text{ K}^{-1}$], h_{fg} [J kg^{-1}], σ [N m^{-1}].

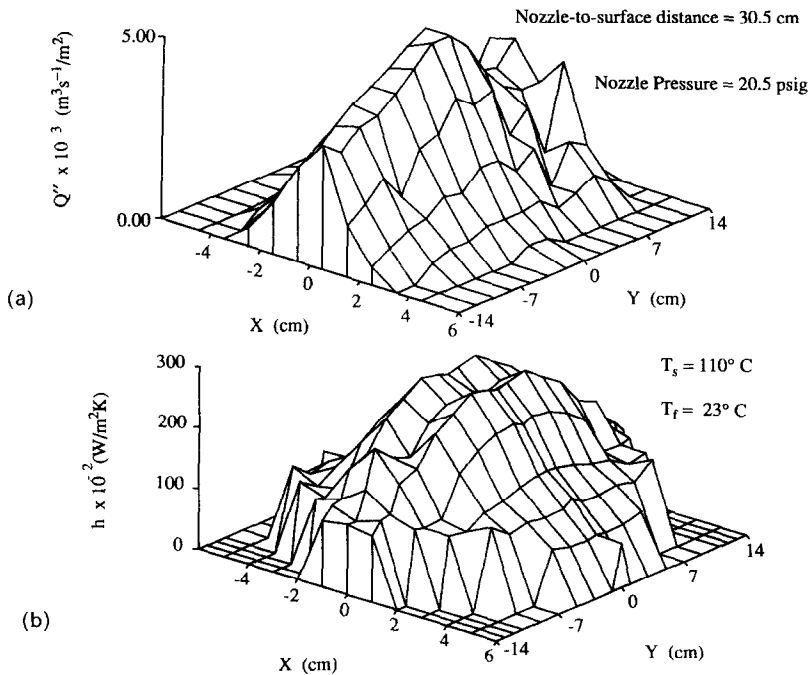


FIG. 2. Variation of (a) volumetric flux and (b) heat transfer coefficient across a spray field.

parameters for drastically different types of sprays currently employed in materials processing? and

(3) Once the spatial distributions of the hydrodynamic parameters are properly characterized, how can these distributions be implemented in the determination of local, instantaneous values of the heat transfer coefficient at the sprayed surfaces of large metallic parts?

The present paper will answer the above questions through both numerical predictions and experimental verification.

2. EXPERIMENTAL METHODS

The present study involved three spray studies: (1) spatial characterization of spray hydrodynamic parameters (volumetric spray flux, mean drop diameter, and mean drop velocity), (2) local spray heat transfer measurements, and (3) quenching of a large rectangular aluminum block. The local heat transfer measurements were first performed to assess the accuracy of existing spray correlations in predicting spatial variations of the heat transfer coefficient in the spray field once the spray hydrodynamic parameters are determined for each location. The spatial variations of the heat transfer coefficient were later employed as spray cooling boundary conditions in the quenching of the aluminum block. Two different types of sprays were examined in order to test the universal validity of the present approach: a *full cone* spray (Spraying Systems 46° FullJet design, $5.3 \times 10^{-5} \text{ m}^3 \text{ s}^{-1}$ (0.84 gpm) at 551 kPa (80.0 psig)), which disperses the liquid flow rate over a circular region of the quenched

surface, and a *hollow cone* spray (Spraying Systems 30° HollowJet design, $3.1 \times 10^{-5} \text{ m}^3 \text{ s}^{-1}$ (0.49 gpm) at 139 kPa (20.0 psig)), which concentrates most of the flow rate towards the outer edge of a circular region.

Flow loop and spray chamber

Figure 3(a) shows the spray chamber inside which all the heat transfer measurements were performed. The chamber was constructed from 2.54 cm thick phenolic and painted internally with water resistant enamel which, along with the use of only stainless steel plumbing in the external flow loop, precluded any contamination of the deionized water used in the tests. Up to 0.11 m^3 of water was preheated to the desired temperature between ambient and 100°C by a 4000 W screw plug immersion heater flanged to the lower side of the spray chamber. The water was supplied through the system by a high pressure stainless steel rotary vane pump. Spray flow rate was adjusted with the aid of two valves, one connected to the nozzle line and the other in a bypass line which routed a portion of the flow back into the chamber. The water advancing to the spray nozzle entered an in-line electric heater followed by a water-cooled heat exchanger, the combination of the two fine tuned the water temperature at the nozzle inlet. Downstream of the heat exchanger was located a $10 \mu\text{m}$ filter followed by a dual range flow meter system having a full-scale accuracy of 2%. The nozzle back pressure was determined by a dial pressure gauge which had a measurement range of 0–689 kPa (0–100 psig). The spray impinged on the hot surface inside the chamber where a portion of the flow evaporated and the balance simply drained

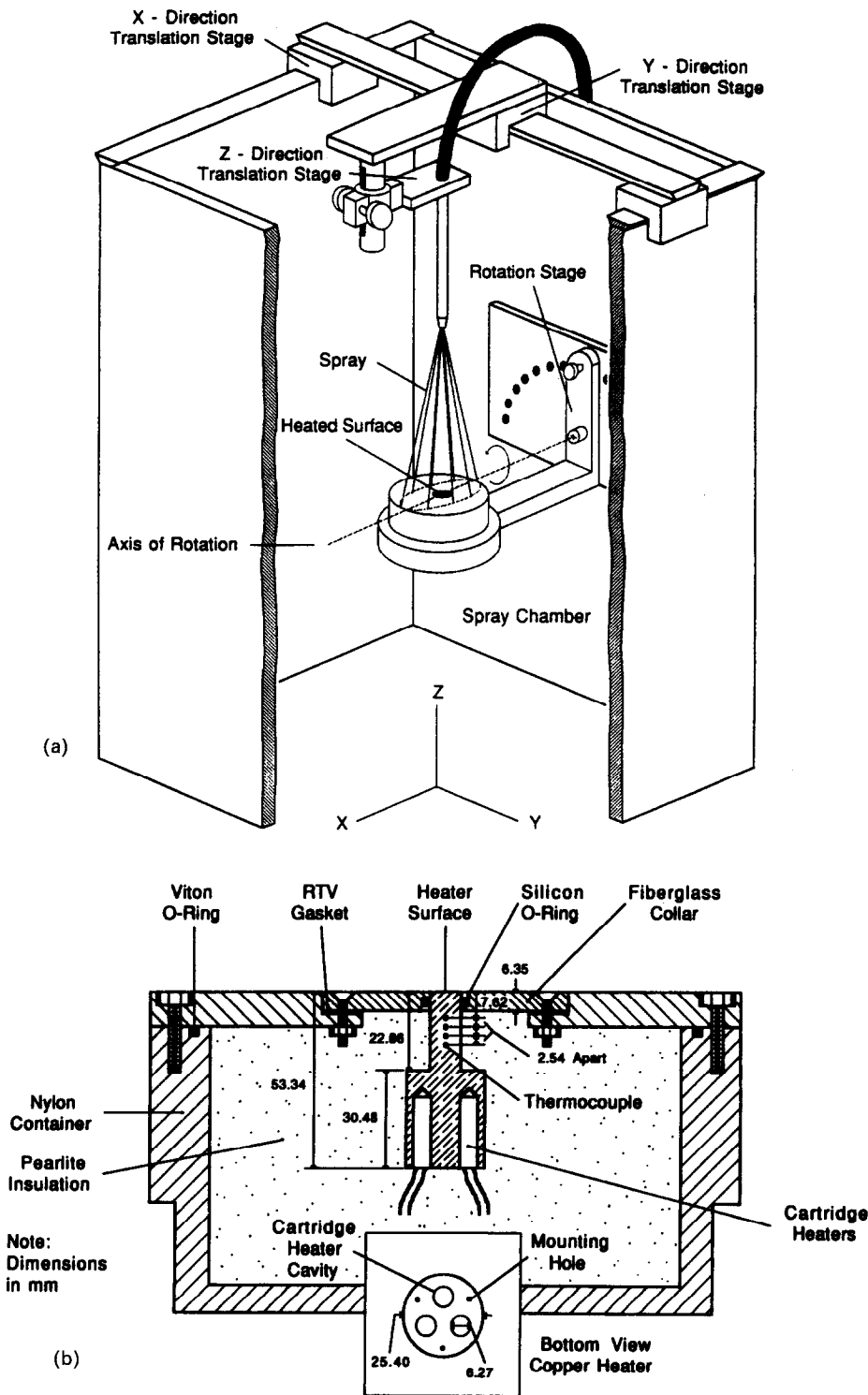


FIG. 3. (a) Cut-away view of spray chamber and (b) sectional view of local heat flux test heater.

off into the bottom of the spray chamber. Throughout the tests, the temperature of the water was monitored in the reservoir, the heat exchanger outlet and the nozzle inlet using type K thermocouples.

Visual access to the spray was made possible through 1.25 cm thick optical grade Lexan windows mounted on three sides of the spray chamber. As

shown in Fig. 3(a), the spray nozzle was mounted on a three degree of freedom translation stage. This system facilitated positioning the nozzle at any X-Y-Z location relative to the test surface, which was mounted at the geometrical center of the spray chamber, to facilitate local measurements of the heat transfer coefficient throughout the spray field.

Local hydrodynamic measurements

Mudawar and Valentine [9] correlated the heat transfer coefficient for sprays with respect to the spray hydrodynamic parameters (i.e. Q'' , $d_{3,2}$, and U_m) which were measured at the center of the spray. In the present investigation, the spatial variations of the same parameters were measured throughout the spray field to examine the suitability of the same correlations to predicting the corresponding variations in the heat transfer coefficient.

Volumetric spray flux, Q'' , was measured by collecting water in a 200 ml graduated cylinder with an inlet area of 1.0 cm² and dividing the volume of collected water by the product of fill time and inlet area. The cylinder inlet was sharpened to reduce any edge effects and the cylinder was placed in the heater bracket so that the cylinder inlet was at the same distance from the spray nozzle as the surface of the test heater.

The Sauter mean diameter was measured at discrete locations within the spray field using a Malvern Particle Sizer available at Spraying Systems (supplier of the spray nozzles used in the present study) particle sizing facilities. This particle sizer utilizes a spatial drop measurement technique by detecting the intensity of light diffracted from a laser beam as the beam is intercepted by the spray drops.

Drop velocities were also measured by the authors at Spraying Systems particle sizing facilities using a model OAP-2D-GA2 two-dimensional gray scale optical array imaging probe. This probe utilizes a temporal measurement technique which consists of illuminating an array of photodiodes by a laser beam and detecting the reduction in light signal due to the shadow cast by the drop during transit in a slicing plane (sampling area) between the laser source and the photodiodes.

Local heat transfer measurements

A high heat flux heater was developed to obtain local heat transfer measurements in nonuniform spray fields. The heater measured heat flux over a 0.5 cm² area which was small enough to detect the sharp spatial gradients in the spray heat flux. As shown in Fig. 3(b), the heater consisted of a calorimeter bar exposed on one end to the spray and heated at its base by three high temperature cartridge heaters. The exposed end of the test heater was flush mounted in a G-7 fiberglass disc which was centered in the lid of a large nylon casing. Four Chromel-Alumel thermocouples, made from 0.076 mm wire, were embedded at 2.54 mm increments along the centerline of the bar through 0.34 mm diameter holes using two-hole ceramic tubes. The spray heat flux was determined from a linear least square fit to the four measured temperatures and the surface temperature was determined by extrapolating the fitted line to the quenched surface.

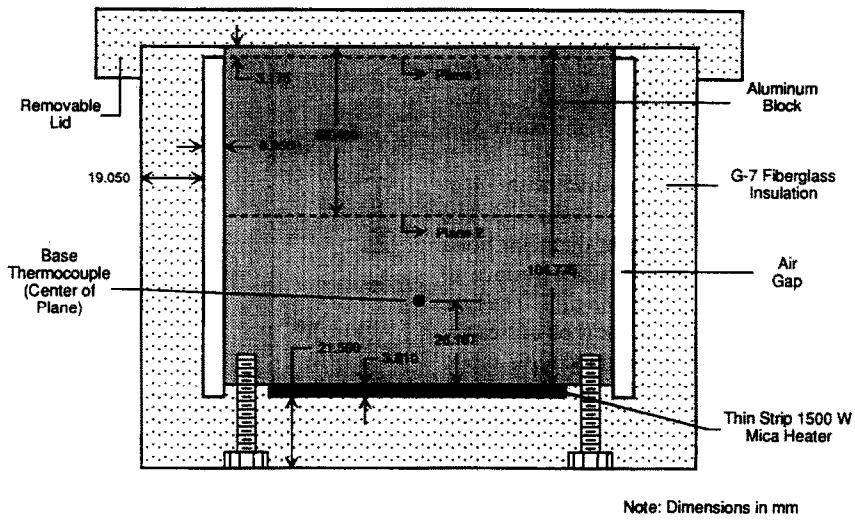
Several test heaters were fabricated, some from oxygen-free copper and others from aluminum. At spray heat fluxes less than about 200 W cm⁻², both

of these high conductivity materials yielded essentially identical boiling curves, consistent with the findings from previous spray studies [9, 10]. However, steady state operation in the film boiling regime resulted in significant oxidation on the surface of the aluminum heater. At high volumetric spray fluxes, the heat flux exceeded 700 W cm⁻², producing very large gradients along the test heater and occasional melting of the heater base. The copper heaters were better suited for these measurements due to a combination of superior corrosion resistance, higher thermal conductivity, and higher melting point. Other details concerning heat flux measurement technique and uncertainties can be found elsewhere [9].

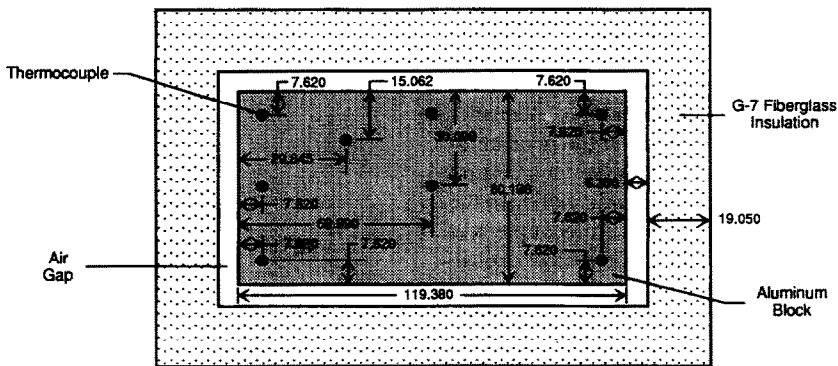
Three dimensional aluminum block for transient quench experiments

A rectangular aluminum block was used to measure the transient temperature response of metallic parts subject to a nonuniform spray cooling boundary much like an actual quenching process. The block geometry and thermal mass were based on a numerical analysis of the quench transient and several design criteria. First, it was desired that the surface of the block exposed to the spray be large enough to exhibit measurable spatial variation in heat flux, due to the spatial gradients in the spray hydrodynamic parameters, yet small enough that no significant portions of the quenched surface be outside the spray field where the heat flux cannot be accurately defined. Second, it was necessary to ensure that the thermal mass of the block was, on one hand, small enough to exhibit strong sensitivity of temperature response to the spray cooling, yet large enough that the block's response was several times slower than the time constant of the thermocouples embedded in the block.

As shown in Fig. 4, the large quenching block consisted of a 6.02 × 11.94 × 10.48 cm³ rectangular aluminum block with a quench area of 71.86 cm². The block was fabricated from 99.4% pure aluminum (1100-O series) for which precise thermal properties were available. The problems encountered with the aluminum calorimeter heaters were not of concern in using the rectangular block since the block was preheated slowly to a fairly uniform initial temperature below the melting point of aluminum before being spray quenched. Heat was supplied to the block by a 1500 W, 0.38 cm thick, high-temperature mica heater which was mechanically clamped to the block underside. A fine layer of boron nitride powder was spread onto the heater to minimize contact resistance with the block. The block and mica heater were enclosed in a rectangular housing made from G-7 insulating fiberglass plastic. Thermal insulation around the block was further enhanced by a 0.64 cm air gap between the aluminum and G-7 walls except for the top surface where the interface between the block and surrounding G-7 was sealed with high temperature RTV silicone rubber. A G-7 lid, fitted with a handle, was machined to cover the top of the block

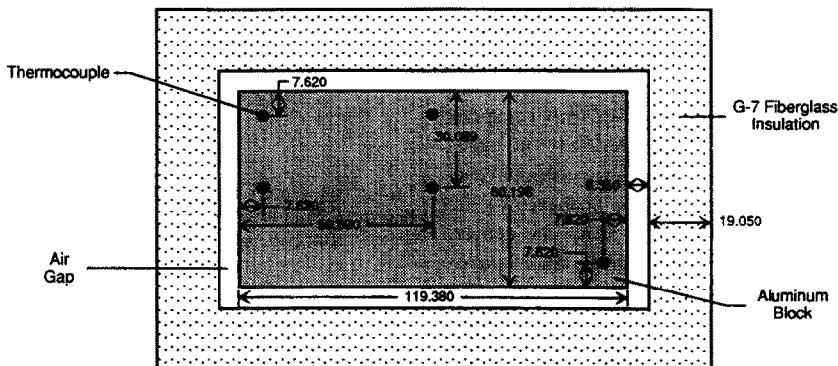


Sectional View



Thermocouple Layout in Plane 1

Note: Dimensions in mm



Thermocouple Layout in Plane 2

FIG. 4. Sectional diagrams of aluminum block.

during preheating of the block and to shelter the aluminum surface from the spray until the desired initial temperature had been reached uniformly throughout the block. The lid could easily and quickly be slid off the surface. This provided a nearly instantaneous application of the spray over the entire surface.

The block temperature was measured with 14 of type T thermocouples made from 0.013 mm wire. The thermocouples were set in 0.071 mm diameter holes drilled in planes parallel to the quenched surface so as to minimize disturbances to the isotherms. The type T thermocouple was selected because it possesses the fastest response of all common thermocouple types. To further enhance the transient response, special care was taken during installation of the thermocouples to ensure excellent contact between the aluminum and the thermocouple bead. The thermocouples were embedded in planes at two different elevations within the block as shown in Fig. 4. Layout of the thermocouple locations was chosen so as to maximize measurement sensitivity to spray cooling non-uniformity. In the plane closest to the surface, temperatures were measured along the centerline and near the corners of the block. One quadrant was finely instrumented to detect any small gradients in the surface heat flux. A smaller number of thermocouples was used in the plane midway through the block since planwise temperature variations were dampened at that depth relative to the quenched surface. An additional thermocouple was embedded at the geometric center of the block 2.6 cm from the bottom. This thermocouple was used both to monitor the block's maximum temperature during heat up and to establish when the block temperature had become uniform. In order to utilize the full speed of the data acquisition system, only a select number of thermocouples was monitored during a given test.

3. RESULTS AND DISCUSSION

Spatial independence of spray cooling correlations

Although Mudawar and Valentine's correlations have been proven accurate at predicting the spray heat flux, these correlations were based only on spray hydrodynamic parameters measured at the geometrical center of the spray. Thus, a key objective of the present study was to examine the accuracy of the same correlations for points away from the center. This was accomplished by measuring the hydrodynamic parameters at select locations, measuring the corresponding boiling curves for the same locations, and comparing the measured heat flux values to those predicted by the correlations.

Figures 5(a) and (b) show boiling curves measured away from the centers of a full cone spray and a hollow cone spray, respectively, compared with predictions using the Mudawar and Valentine correlations based on local values of the hydrodynamic parameters. Both figures demonstrate favorable agreement between the predicted and measured values in the transition boil-

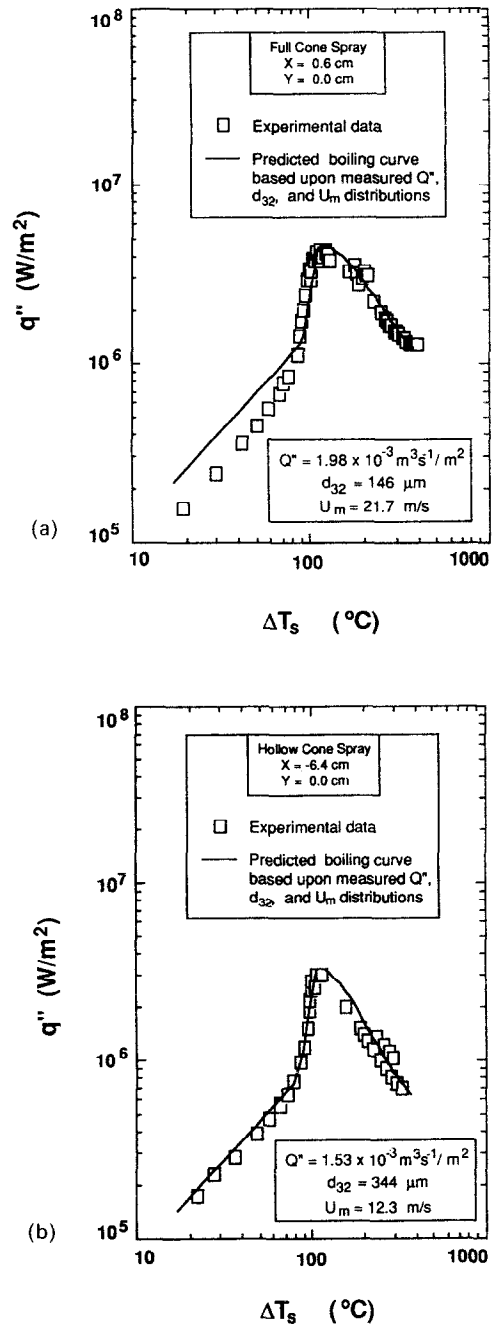


FIG. 5. Measured boiling curve compared to predictions based on Mudawar and Valentine's correlations [9] for (a) full cone spray and (b) hollow cone spray.

ing and nucleate boiling regimes, alas with some departure in the single-phase regime for the full cone spray. Visual observation revealed the underlying mechanism responsible for the departure from the predictions prevalent in the single-phase regime. In the local spray heat flux measurements, only the small area of the test heater was undergoing boiling as a liquid film emanating from the center of the spray increased in flow rate as it captured the spray drops while flowing radially outward along the large

unheated area surrounding the test heater. During both transition and nucleate boiling, drop impingement and the ensuing vigorous boiling were observed to disrupt the liquid run-off, creating conditions which were fairly insensitive to the run-off. However, as boiling subsided, the conditions on the heater surface became much more sensitive to the liquid run-off. Fortunately, as mentioned in the Introduction, the single-phase regime is of little significance to metallurgical structure and resulting mechanical properties of metallic parts following heat treating. Needless to say, the liquid run-off flow rate in the local test heater studies is much greater than would be incurred during the quenching of an entire surface. The results shown in Figs. 5(a) and (b) clearly demonstrate that the local spray cooling correlations developed by Mudawar and Valentine for the transition and film boiling regimes are spatially independent and can, therefore, be used to predict spatial variations of heat transfer coefficient once the hydrodynamic parameters of the spray have been spatially mapped.

Determination of spatial distribution functions for the hydrodynamic parameters

Since detailed spatial mapping of drop velocity and drop diameter is both time consuming and cost prohibitive to most heat treating operations, a more practical approach to characterizing the spray hydrodynamic parameters was pursued. First, these parameters were measured at discrete locations in the spray field as shown for the Q'' values in Figs. 6(a) and (b). An asymmetric, three dimensional distribution function of the form

$$\Psi(X, Y) = A_0 \exp(A_1 X + A_2 Y + A_3 X^2 + A_4 XY + A_5 Y^2) \quad (1)$$

was found to possess the flexibility of fitting the measured values of Q'' , d_{32} , and U_m while allowing for asymmetry in the distributions of these parameters due to any minute imperfections in the fabrication of the spray nozzle. The constants A_0, A_1, \dots, A_5 in equation (1) were determined by a least square fit to a minimum of six discrete measurements of each of the three hydrodynamic parameters. Equation (1) was equally successful at fitting hollow cone data, with a higher concentration of drops away from the center, as it did full cone data, where volumetric spray flux assumes its maximum value at the center and decays towards the outer edge of the spray field. The sprays examined in the present study assumed peak or minimum volumetric spray flux values (depending on the type of nozzles used) at locations slightly skewed from the geometrical center. This skewness produced a measurable shift in the cooling uniformity for some of the spray nozzles, thus the importance of employing an asymmetric distribution function. Drop diameter and drop velocity distributions, on the other hand, manifested only small spatial changes, yet equation (1) demonstrated flexibility at fitting these fairly flat

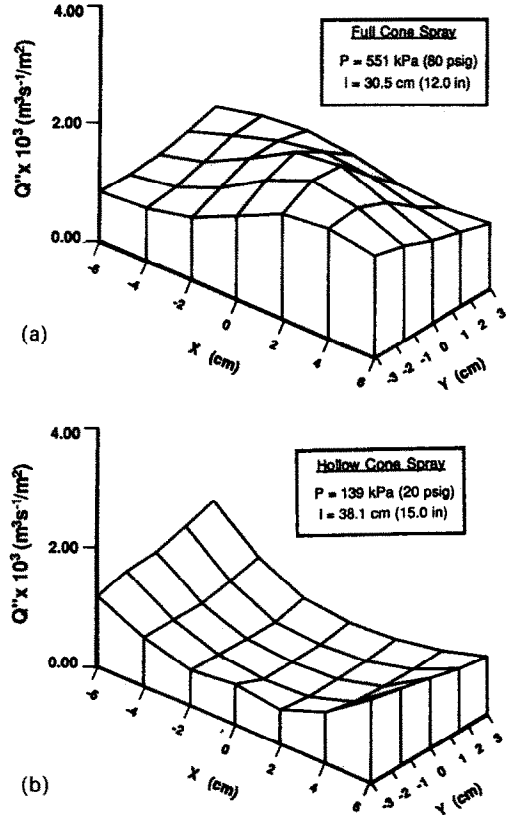


FIG. 6. Measured spatial distributions of Q'' for (a) full cone spray and (b) hollow cone spray.

distributions as well. The fitted distributions of Q'' , d_{32} , and U_m for the full cone spray and hollow cone spray are shown in Figs. 7(a) and (b), respectively.

Since the values of the spray hydrodynamic parameters can be determined at any point in the spray field with the aid of the fitted spatial distribution functions, it is possible to utilize these functions with the Mudawar and Valentine correlations in order to predict the spatial distribution of the spray heat transfer coefficient. The next section will examine the validity of this approach in predicting the temperature response of the large aluminum block as it is quenched on one side by a nonuniform spray.

4. NUMERICAL SIMULATION

The transient, three dimensional response of the aluminum block to the quench was simulated using a finite difference technique. The numerical domain measured $6.02 \times 11.94 \times 10.48 \text{ cm}^3$, the dimensions of the aluminum block itself. This domain was discretized nonuniformly in each of the X , Y , and Z coordinates, where X and Y are measured from the axis of the block along the length and width of the quenched surface, respectively, and Z is measured normal to the quenched surface. Grids in the three directions were first defined to coincide with thermocouple locations. Afterwards, grids were added to smooth out the discretized domain, making it very

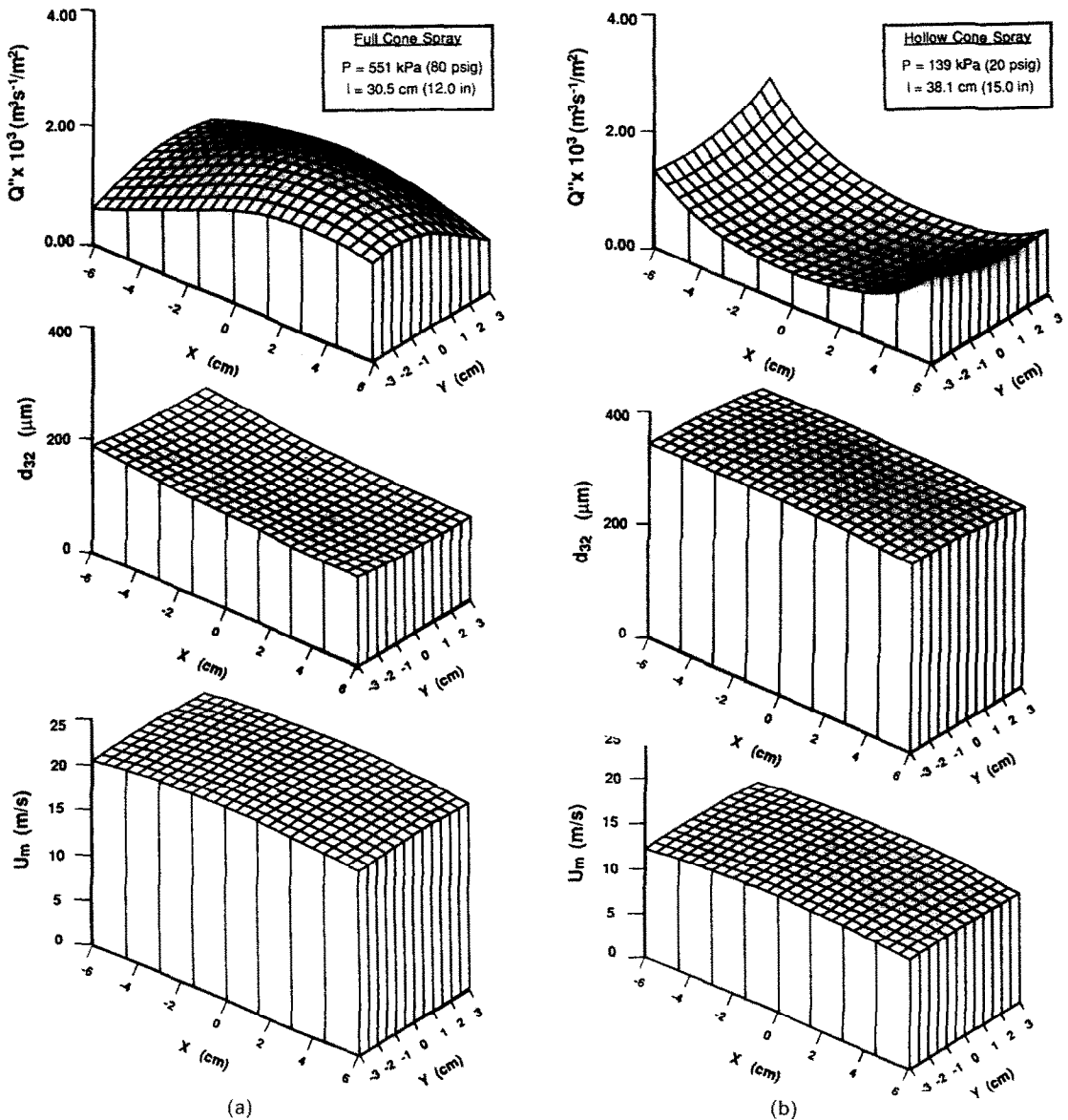


FIG. 7. Fitted spatial distributions of Q'' , d_{32} , and U_m for (a) full cone spray and (b) hollow cone spray.

finely spaced near the sprayed surface in the Z direction, where the largest temperature gradients were encountered, and as equally spaced as possible in X and Y directions. The time domain was discretized using a power law function since very fine time increments were needed for the transition boiling regimes, where temperatures changed very rapidly. The temperature response was predicted by solving the heat diffusion equation

$$\frac{\partial^2 T}{\partial X^2} + \frac{\partial^2 T}{\partial Y^2} + \frac{\partial^2 T}{\partial Z^2} = \frac{1}{\alpha} \frac{\partial T}{\partial t} \quad (2)$$

after approximating the partial derivatives with finite difference equations using PHOENICS. The properties of aluminum were input as functions of temperature to accurately model any appreciable vari-

ations of these properties during the simulated quench. The initial condition for the numerical simulation was a uniform block temperature equal to the temperature measured at the onset of the quench. Two numerical simulations were performed where the aluminum block was subjected to either a full cone spray or a hollow cone spray.

The plane of grid points nearest to the sprayed surface ($Z = 0$) was located only 0.05 mm away from the surface. The surface temperature, which is not readily calculated by PHOENICS, was determined from a thermal resistance circuit consisting of a conduction resistance in the Z direction between the node closest to the surface and the surface itself in series with a convective resistance between the surface and the spray. Radiation effects were neglected since the heat

transfer coefficient due to radiation alone (based on a surface temperature of 200°C and an emissivity of 0.1) was less than 0.2% of the lowest value for the heat transfer coefficient due to spray convection. In determining the local, instantaneous spray convection coefficient, local values of the spray hydrodynamic parameters (Q'' , d_{32} , and U_m) were first determined from the spatial distribution functions given in Figs. 7(a) and (b). These values were then substituted in the

Mudawar and Valentine correlations, resulting in a unique boiling curve for every location on the quenched surface. The individual boiling curves were saved in computer memory so that, for the remainder of the numerical simulation, knowledge of the surface temperature at a given surface location was sufficient to calculate the instantaneous convection coefficient for that location.

The other five sides of the aluminum block were

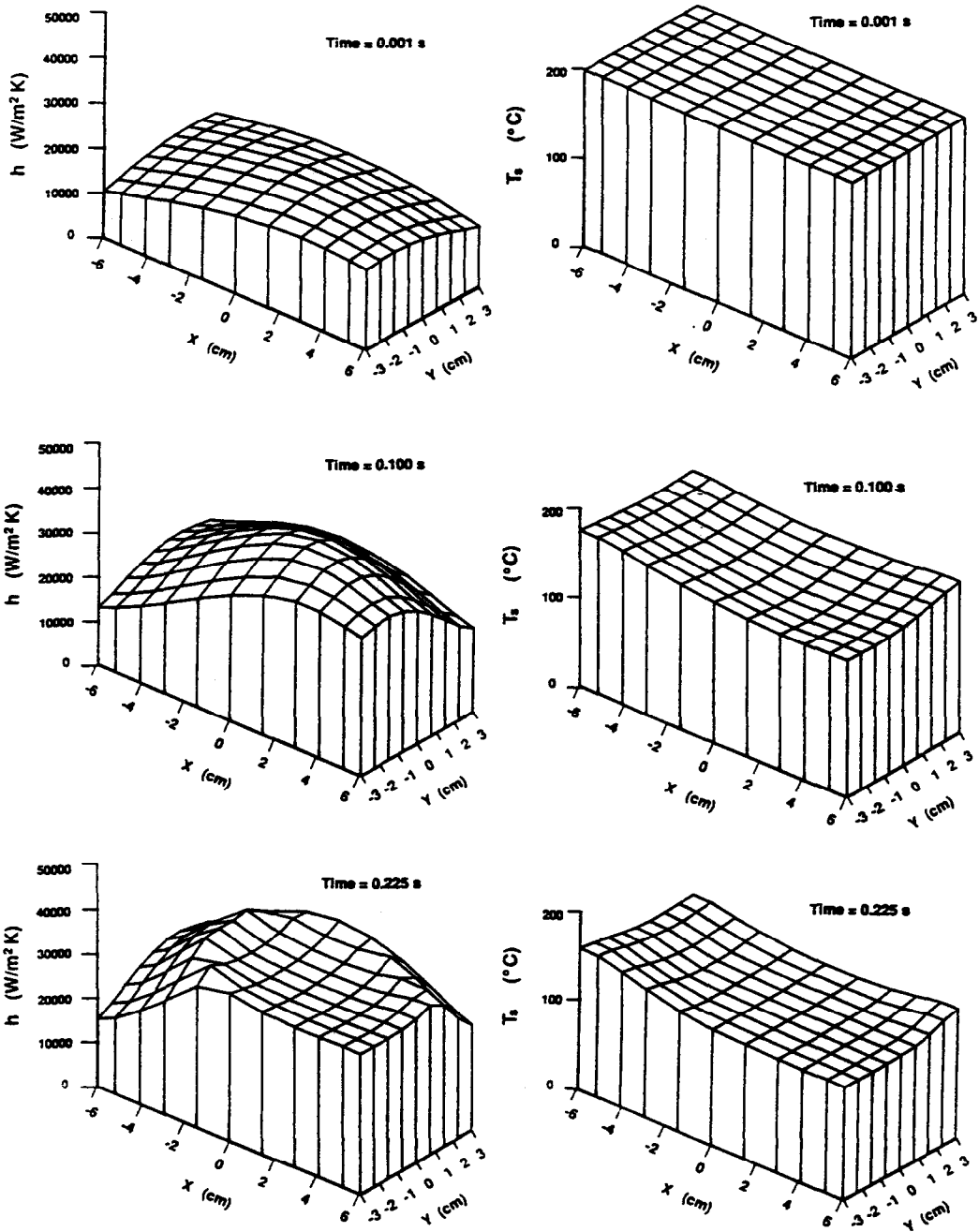


FIG. 8. Spatial variations of heat transfer coefficient and surface temperature at different times during simulated quenching by full cone spray.

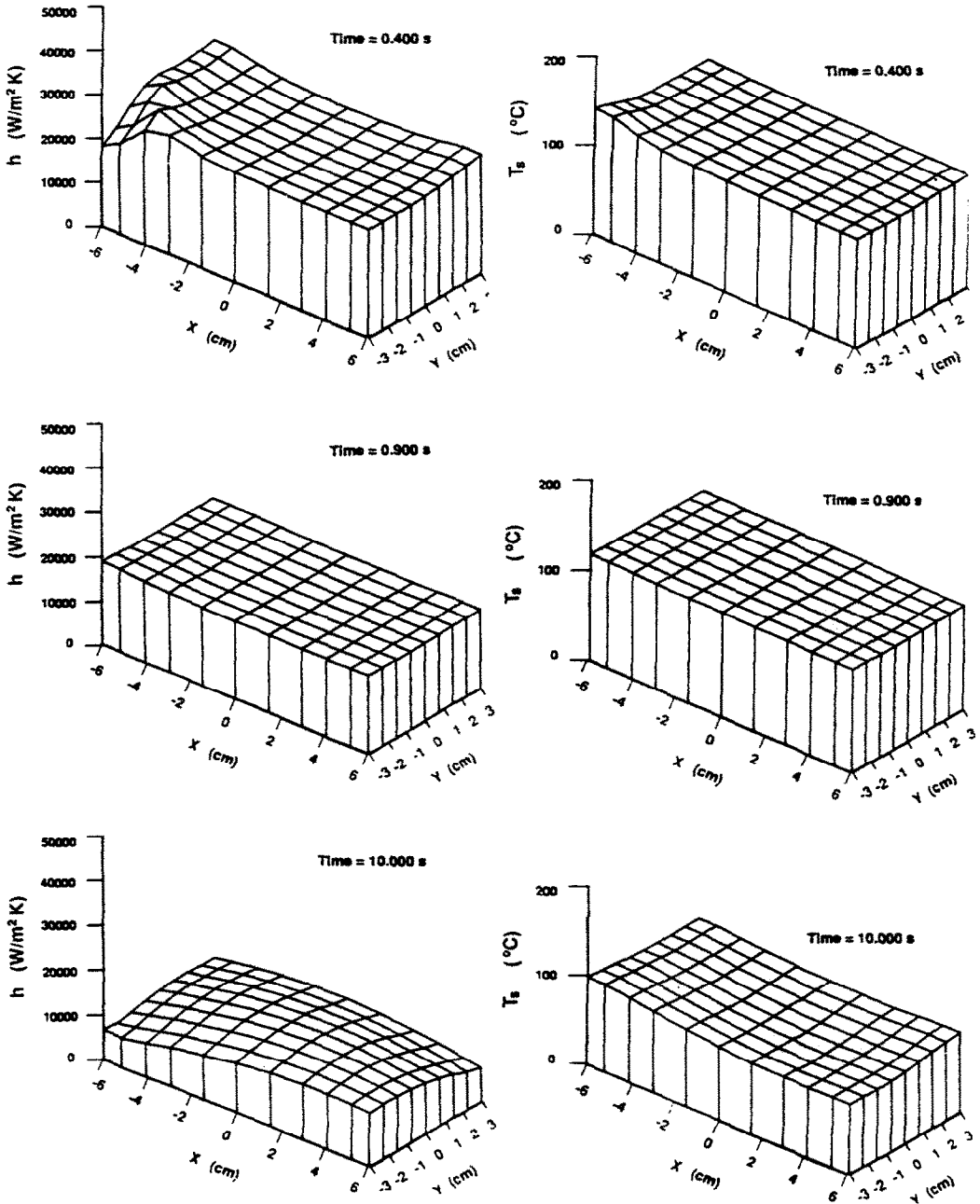


FIG. 8.—Continued.

insulated in the actual experiment. However, the insulation was less than perfect, thus some heat was lost through these boundaries. A simplified one dimensional numerical model of heat loss through the air gap and fiberglass casing showed that, within the approximately 60 s duration of the quench, the five non-quenched sides of the aluminum block experienced insignificant heat loss relative to the quenched surface. Therefore, these boundaries were assumed perfectly insulated in the numerical simulation.

One method of tracing the temperature response of the block is to examine the variations of the spray heat transfer coefficient and temperature across the quenched surface ($Z = 0$) at different times during the transient. Such variations are shown for the full cone spray in Fig. 8. A brief duration following commencement of the quench, $t = 0.001$ s, the asymmetry in the volumetric spray flux of the nozzle used, Fig. 7(a), quickly manifests itself in a corresponding asymmetry in the heat transfer coefficient distribution. The

large value of Q'' near the center greatly increases h in that region relative to the edges, resulting in a faster temperature response near the center. At $t = 0.225$ s, the central region of the surface has already entered the nucleate boiling regime while the edges endured transition boiling. The heat transfer coefficient in the

nucleate boiling region increases in magnitude but becomes flatter since the Mudawar and Valentine correlations show h is insensitive to variations in volumetric spray flux in the nucleate boiling regime. The central 'quenched' region assumes a front which spreads outward from the center in the direction of

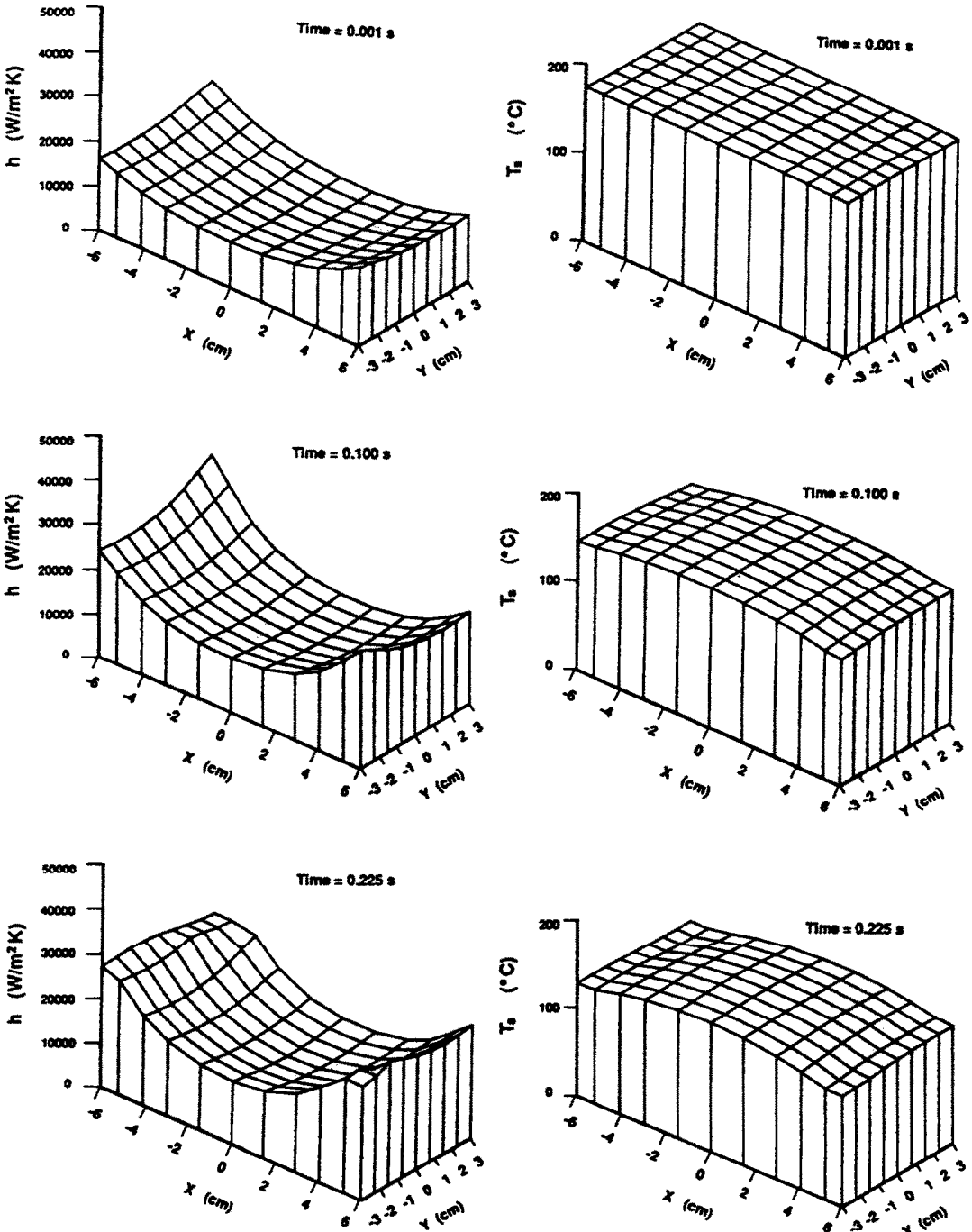


FIG. 9. Spatial variations of heat transfer coefficient and surface temperature at different times during simulated quenching by hollow cone spray.

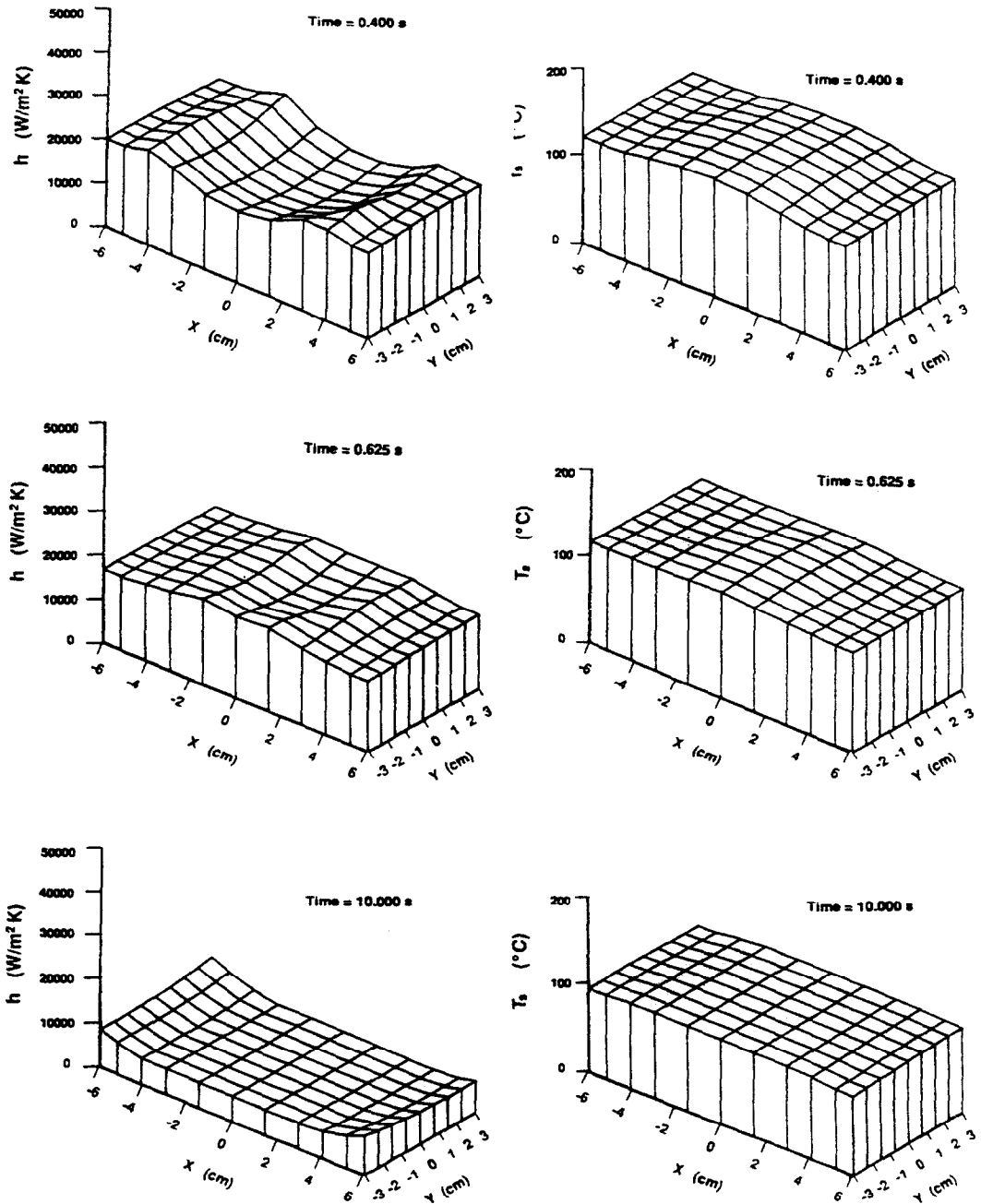


FIG. 9.—Continued.

high to low volumetric spray flux as shown in the heat transfer coefficient distribution at $t = 0.45$ s. As nucleate boiling completely subsides and the single-phase cooling regime is established over the entire surface, $t = 10$ s, the value of h decreases drastically and recovers its sensitivity to the spatial variation in volumetric flux as predicted from the Mudawar and Valentine correlation for the single-phase cooling regime.

Figure 9 shows a similar time series of the spatial variations of h and T_s predicted for the hollow cone

spray. As expected, the outer edges of the sprayed surface quench the fastest and enter the nucleate boiling regime earlier, as shown in Fig. 9 for $t = 0.225$ s, due to the greater volumetric spray flux in those regions relative to the center. The quench front propagates with time toward the center, spreading nucleate boiling across the surface which finally subsides into the single-phase cooling regime.

Figure 10(a) shows for the full cone spray a comparison of measured and predicted temperatures along the central axis of the block ($X = 0, Y = 0$) and

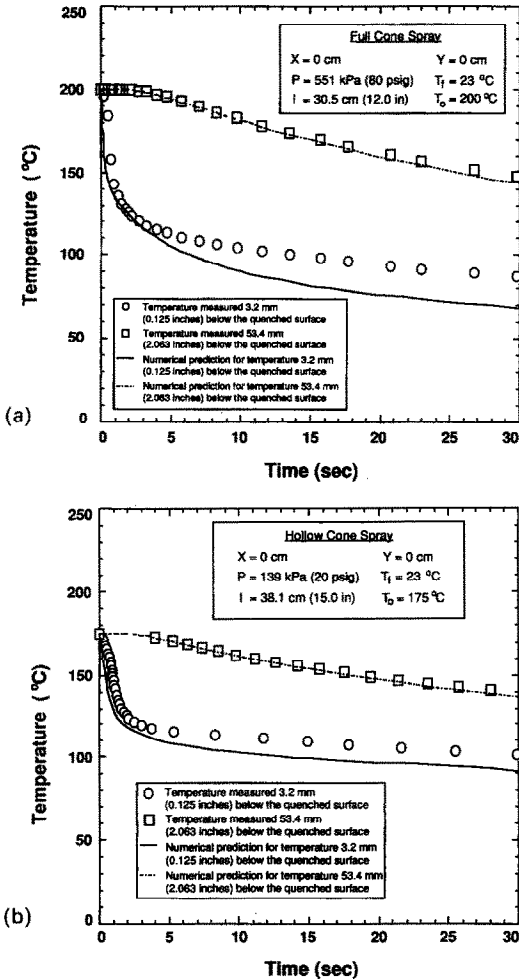


FIG. 10. Temperature response of central axis of rectangular block to (a) full cone spray and (b) hollow cone spray.

distances of 3.2 mm and 53.4 mm below the quenched surface. As expected, the response of the point away from the quenched surface was considerably delayed relative to the point closer to the surface. Good predictions resulted at both locations throughout the transition boiling and nucleate boiling regimes. Deviation between the predicted and measured temperatures at $Z = 3.2$ mm coincided approximately with the onset of single-phase cooling, the response at $Z = 53.4$ mm was too damped to manifest any significant deviation. The deviation between the predicted and measured temperatures in the single-phase regime is postulated to be the result of several effects associated with liquid run-off. The vigorous vapor effusion in both the transition boiling and nucleate boiling regimes tends to evaporate the spray drops rapidly following impact. However, in the single-phase cooling regime, each drop deforms upon impact spreading a thin film which quickly coalesces with films formed by adjacent drops into a much thicker liquid run-off film. The run-off film emanates from the center of the quenched surface and, as it moves toward the edges of the surface, greatly influences the

impact of drops away from the center. These results indicate the present method of determining the spatial distribution of the spray heat transfer coefficient is very accurate over the temperature range most crucial to the metallurgical structure of the quenched part, the transition boiling and nucleate boiling regimes. However, the present method suffers some loss of accuracy in the final stage of quenching, single-phase cooling regime.

Figure 10(b) compares the predicted and measured response for the hollow cone spray at the same locations as those of Fig. 10(a). These results show good agreement between the predicted and measured values including the single-phase cooling regime. One reason for the better agreement in this regime compared to the full cone spray is the small flow rate of the run-off liquid film emanating from the center of the hollow cone spray since most of the spray flux is concentrated away from the center. Figure 11(a) compares the predicted and measured temperatures 3.2 mm below the center of the surface subjected to the hollow cone spray ($X = 0, Y = 0$) and at the same

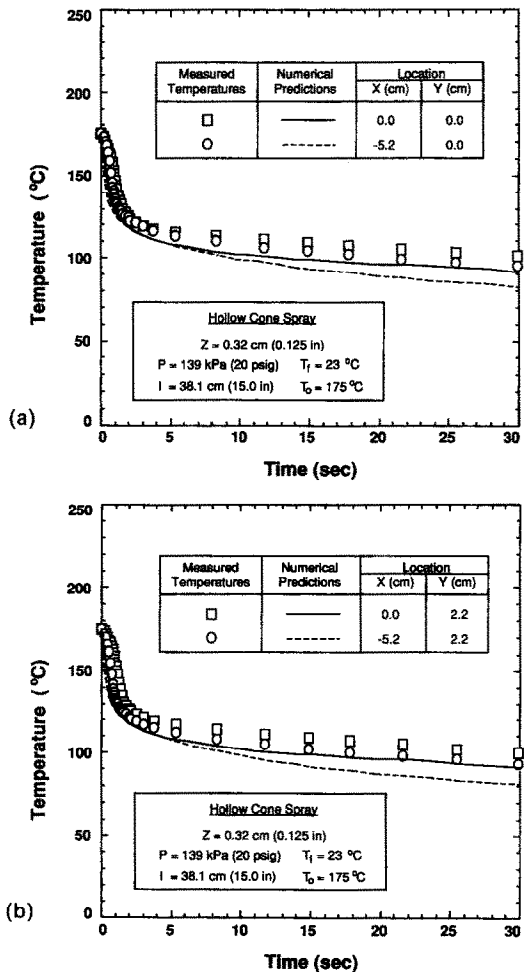


FIG. 11. Temperature response of (a) side relative to center and of (b) another side and corner of the rectangular block to hollow cone spray.

distance below one side of the surface ($X = -5.2$ cm, $Y = 0$). Both the data and the numerical model show the faster response near the side relative to the center due to a greater volumetric spray flux toward the side. Figure 11(b) shows a comparison of the predicted and measured temperatures at 3.2 mm below two other surface locations, one towards the other side ($X = 0$, $Y = 2.2$ cm) and the other toward the corner ($X = -5.2$ cm, $Y = 2.2$ mm). Figure 11(b) displays the same trends depicted in Fig. 11(a), some deviation of predicted from measured temperatures in the single-phase cooling regime and a faster response at points situated farther from the center of the sprayed surface.

5. CONCLUSIONS

This study aimed at developing a method for predicting the temperature response of metallic parts to spray quenching below the film boiling regime. Key conclusions from the study are as follows:

(1) Existing spray quenching correlations, which were developed from measurements at the geometrical center of water sprays, were found to work well at any other location within the spray field once the hydrodynamic parameters of the spray (Q'' , d_{32} , and U_m) are determined for these locations. The correlations worked well for sprays with drastically different patterns, full cone sprays and hollow cone sprays, both in the transition boiling and nucleate boiling regimes, but were less accurate in the single-phase regime because of liquid run-off effects.

(2) Using a small number of discrete measurements of the hydrodynamic parameters across the spray field, it is possible to construct accurate spatial distribution functions for these parameters. Combined with the local spray quenching correlations, the spatial distribution functions of the hydrodynamic parameters can be used to construct corresponding spatial distribution functions for the spray heat transfer coefficient at every instant during the quench.

(3) The new method of mapping the heat transfer coefficient across the spray field is very successful at predicting the temperature response of large metallic

parts to spray quenching both in the transition boiling and nucleate boiling regimes.

Acknowledgements—Financial support of this work by the Purdue University Engineering Research Center for Intelligent Manufacturing Systems is gratefully appreciated. The authors also thank Messrs Jerry Hagers and Rudolph Schick of Spraying Systems Company for their valuable technical assistance.

REFERENCES

1. T. A. Deiters and I. Mudawar, Optimization of spray quenching for aluminum extrusion, forging, or continuous casting, *ASM J. Heat Treating* **7**, 9–18 (1989).
2. J. K. Brimacombe, P. K. Agarwal, L. A. Baptista, S. Hibbins and B. Prabhakar, Spray cooling in the continuous casting of steel, *Proc. 63rd National Open Hearth and Basic Oxygen Steel Conf.*, Washington, D.C., pp. 235–252 (1980).
3. L. Bolle and J. C. Moureau, Spray cooling of hot surfaces: a description of the dispersed phase and a parametric study of heat transfer results. In *Two-Phase Flows and Heat Transfer*, Vol. 3, pp. 1327–1346, *Proc. NATO Advanced Study Institute*, Washington, D.C. (1977).
4. L. Bolle and J. C. Moureau, Experimental study of heat transfer by spray cooling, *Proc. Int. Conf. on Heat and Mass Transfer in Metallurgical Processes*, Dubrovnik, Yugoslavia, pp. 527–534 (1979).
5. K. Sasaki, Y. Sugitani and M. Kawasaki, Heat transfer in spray cooling on hot surface, *Testu-To-Hagane* **65**, 90–96 (1979).
6. H. Muller and R. Jeschar, Untersuchung des Wärmeübergangs an einer simulierten Sekundärkühlzone beim Strömungsverfahren, *Arch. eisenhüttenwes* **44**, 589–594 (1973).
7. L. Ubanovich, V. Goryaninov, V. Sevost'yanov, Y. Boev, V. Niskovskikh, A. Grachev, A. Sevost'yanov and V. Gur'ev, Spray cooling of high-temperature metal surfaces with high water pressures, *Steel in the USSR* **11**, 184–186 (1981).
8. U. Reiners, R. Jeschar, R. Scholz, D. Zebrowski and W. Reichelt, A measuring method for quick determination of local heat transfer coefficients in spray cooling within the range of stable film boiling, *Steel Res.* **56**, 239–246 (1985).
9. I. Mudawar and W. S. Valentine, Determination of the local quench curve for spray-cooled metallic surfaces, *ASM J. Heat Treating* **7**, 107–121 (1989).
10. K. J. Baumeister and F. F. Simon, Leidenfrost temperature: its correlation for liquid metals, cryogenics, hydrocarbons and water, *Trans. ASME, J. Heat Transfer* 166–176 (1973).